energies

MDPI

Article

Heat Dissipation in Variable Underground Power Cable Beddings: Experiences from a Real Scale Field Experiment

Christoph Verschaffel-Drefke [1,2,*], Markus Schedel [1,2], Constantin Balzer [2,3], Volker Hinrichsen [2,3] and Ingo Sass [1,2]

[1] Geothermal Science and Technology, Department of Materials and Earth Sciences, Technical University of Darmstadt, Schnittspahnstr. 9, 64287 Darmstadt, Germany; schedel@geo.tu-darmstadt.de (M.S.); sass@geo.tu-darmstadt.de (I.S.)
[2] Darmstadt Graduate School of Excellence Energy Science and Engineering, Technical University of Darmstadt, Otto-Berndt-Str. 3, 64287 Darmstadt, Germany; balzer@hst.tu-darmstadt.de (C.B.); hinrichsen@hst.tu-darmstadt.de (V.H.)
[3] High-Voltage Laboratories, Department of Electrical Engineering and Information Technology, Technical University of Darmstadt, Fraunhoferstr. 4, 64283 Darmstadt, Germany
* Correspondence: drefke@geo.tu-darmstadt.de

Abstract: To prevent accelerated thermal aging or insulation faults in cable systems due to overheating, the current carrying capacity is usually limited by specific conductor temperatures. As the heat produced during the operation of underground cables has to be dissipated to the environment, the actual current carrying capacity of a power cable system is primarily dependent on the thermal properties of the surrounding porous bedding material and soil. To investigate the heat dissipation processes around buried power cables of real scale and with realistic electric loading, a field experiment consisting of a main field with various cable configurations, laid in four different bedding materials, and a side field with additional cable trenches for thermally enhanced bedding materials and protection pipe systems was planned and constructed. The experimental results present the strong influences of the different bedding materials on the maximum cable ampacity. Alongside the importance of the basic thermal properties, the influence of the bedding's hydraulic properties, especially on the drying and rewetting effects, were observed. Furthermore, an increase in ampacity between 25% and 35% was determined for a cable system in a duct filled with an artificial grouting material compared to a common air-filled ducted system.

Keywords: ampacity rating; bedding material; field experiment; heat dissipation; thermal cable rating; underground power cable

Citation: Verschaffel-Drefke, C.; Schedel, M.; Balzer, C.; Hinrichsen, V.; Sass, I. Heat Dissipation in Variable Underground Power Cable Beddings: Experiences from a Real Scale Field Experiment. *Energies* **2021**, *14*, 7189. https://doi.org/10.3390/en14217189

Academic Editor: Gian Giuseppe Soma

Received: 6 October 2021
Accepted: 28 October 2021
Published: 2 November 2021

1. Introduction

The reliable function of the electrical energy supply is one of the most important parameters for both an improved quality of life of the population and for the economic growth of countries worldwide [1]. For this purpose, the distribution systems of electrical energy require a maximum transmission capacity to work economically efficiently as well as to ensure a maximum supply safety. To guarantee these qualities, the electric grid infrastructure has to be extended or modified in many countries within the next decades [2,3]. In developing countries, this is necessary to avoid an overload in the grid due to the rapidly growing industries and changes in the population structure. In industrialized countries, particularly in Germany, an increased decentralization of electrical energy production and an increasing number of fluctuating regenerative energy sources, such as wind or solar energy systems, leads to significant changes in the load amplitude and dynamic faced by cable systems. For reasons of acceptance or for reasons related to structural engineering, the majority of these expansions cannot be executed as pure overhead transmission lines but need to be conducted using underground power cables [4–6].

For an efficient integration of renewable energies and the avoidance of over-dimensioning cable systems, the thermal current carrying capacity must be precisely determinable even under highly fluctuating load regimes. Especially since further dimensioning restrictions, such as the maximum voltage drop within a distribution grid, are increasingly controlled by new technologies such as transformers, with voltage regulation performed by tap changers, an adequate thermal current rating becomes essential for an efficient cable system operation [7].

1.1. Thermal Cable Rating

In order to prevent insulation faults in cable systems due to overheating, the current carrying capacity is limited by specific conductor temperatures. As the heat produced by the cables has to be dissipated to the environment, the actual performance of a buried power cable system depends on the thermal properties of the cable materials and the cable's surroundings [8].

In order to calculate the current carrying capacity (often denoted as the ampacity rating), international standards such as those of the International Electrotechnical Commission (IEC) suggest primarily analytical methods using equivalent thermal networks, principally based on the work of [9]. Cable rating calculations according to the IEC standards [10,11] set current limits regarding the type and geometry of a cable, the number of cumulated cable systems, the thermal conductivity, and the temperature of the cable's surroundings as well as the cable loading during operation. Specifically with regard to the cable surrounding material, simplifications are recommended.

When using the international standards, two approaches can be distinguished for the thermal consideration of the medium surrounding the cable, whereby the earth's surface is always considered as the decisive heat sink for the cable losses. In the simplest case, the bedding material or the soil surrounding the cable is considered to be a homogeneous material with constant material properties. However, in the 1960s it was already discovered that this simplified approach might lead to undersized cable sections resulting in soil drying out and thus to equipment failure due to overheating [12]. This is not surprising, as the thermal properties of porous media such as cable beddings are strongly dependent on the water content and can therefore only be regarded as spatially and temporally constant in limited situations, especially in the case of additional thermal gradients caused by the cable operation. As a consequence of the physical effects of coupled heat and mass transport, if the soil moisture content falls below a critical level at which the capillary water transport collapses, local drying-out may occur within the area of the heat source or cable [8]. As the description of these effects in models such as those proposed in [13], is very complex, approaches for a simplified implementation of partial soil drying in the existing calculation methods of the standards were developed in the 1970s [12]. In reports of the CIGRE committee [14,15], the so-called two-zone model was established for the consideration of partial soil drying-out. The model is based on the subdivision of the cable bedding into two distinct areas (wet and dry) for stationary and cyclical loading scenarios and is still a valid technique used today.

The two-zone model of partial soil drying assumes that the heat transport is solely conductive, and that the undisturbed cable bedding initially has a homogeneous thermal conductivity [12]. When a critical temperature (often called the critical temperature rise) is exceeded, a sudden change in thermal conductivity to that of the completely dry soil is assumed and a distinction of the thermal resistance of the bedding is made. Hence, it is assumed that the isotherms surrounding a cable in operation also represent isolines of the soil moisture. To apply the two-zone model, three material characteristics (thermal conductivity of wet and dry material as well as critical temperature rise) of the cable bedding must first be known and should be determined experimentally if possible [8]. However, the determination of the critical temperature rise is quite complex and strongly dependent on the applied boundary conditions. Therefore, although a corresponding

approach is recommended in [16], constant table values are used for this parameter in practice, almost without exception.

Thus, in contrast to the generally well-known thermal properties of the cable construction elements, the characteristics of the surrounding cable bedding and soil which are necessary for the ampacity rating usually have a comparatively high uncertainty.

1.2. Investigation of the Bedding's Influence on the Heat Dissipation of Underground Power Cables

The heat transport in porous materials such as buried power cable beddings is primarily performed by conduction in a dry and a water saturated state. Furthermore, particularly directly around the cable, a convective mass flow of the mobile phases (i.e., the soil air and water contained in the pore space) as well as the latent heat of water vapor can contribute to the overall heat transfer. Thus, in unsaturated porous media such as soil the total heat flux can be described as a sum of conductive, convective, and latent heat transport. The latter two can even significantly exceed the proportion of conductive heat transport. Heat transport due to radiation is a decisive issue at the soil surface, whereas it can be neglected in the soil profile [17,18]. The mentioned convective movements of water or air in the pore space follow the pressure, concentration, or density gradients. With increasing temperature gradients, an increased evaporation of liquid water occurs near the cable, which acts as the heat source, and the water vapor condensates at a further distance from it. The occurrence of energy transfer at these phase changes is described as latent heat transport.

While conventional methods for calculating the cable ampacity only consider the conductive heat transport, an integration of coupled heat and mass transport processes in these calculations might allow for significant optimizations. Using numerical studies, it is possible to investigate and quantify the influence of water and vapor movement on different heat transport processes in unsaturated porous media and on the overall heat transport at thermal gradients [19–21]. However, it is usually not desirable, in practical applications, to execute these comparatively complex calculations to determine and distinguish the different heat transport processes as well as to quantify their proportion on the overall heat transport. For simplification, a common and practical method is to consider only heat transfer by conduction, using an apparent thermal conductivity that merges all relevant heat transport processes [22,23].

Due to the increasing relevance of the topic, particularly in Central-Europe, several—predominantly numerical—studies recently investigated heat dissipation processes of underground cables and the influence of soil/bedding-properties on the ampacity ranking (e.g., [24–26]). Most of the studies have a strong theoretical or numerical approach and tend to display a lack of adequate experimental data for the transfer of the results to full-scale application. In addition, experiments are usually not designed in scale or a relevant physical environment, and operating conditions are neglected in order to simplify the experimental setups and define the known boundary conditions. Furthermore, besides the numerous (often down scaled) laboratory studies, only a few real scale field experiments exist to investigate the thermal field around buried power cables.

Unfortunately, due to the strenuous technical effort, real power cables are not used for most studies, instead, alternative heat sources are used. Some studies [27] used heating pipes and fluids such as water or oil as the heat carrier medium, although there are some significant disadvantages in this method, such as the potential of inhomogeneous longitudinal heat propagation compared to direct electrical heating that uses wires or cables. In most studies, pipes with electrical heating were chosen to act as dummy cables [28–30]. Only a few of the experimental setups are known to have used real power cables [31,32]. However, all of them use parts of cable routes that are in operation or under construction. This results in certain restrictions in the design and specifically in the operation of the test routes, since the cable load cannot be freely selected but corresponds to the regular grid load. Thus, the cables are usually operated significantly below their maximum capacity and heat dissipation can only be investigated in very few situations. Studies such as that of a connecting cable route between two substations in Osterath (Germany) are exceptions.

Prior to the beginning of regular operation of the Osterath cable route, tests were carried out for a limited period of approximately two years using a constant technical maximum load on HV cables in four bedding materials [33]. However, different cable configurations or dynamic loads were not investigated.

Thus, from the authors' point of view, none of the previous experiments fulfilled the requirements for an investigation of heat dissipation processes of underground power cables in different bedding materials in real scale. An experimental setup that enables investigations on various cables and cable arrangements in different bedding materials and soils under natural conditions as well as various load scenarios is required. Therefore, a real scale field experiment was built in 2012–2013 at TU Darmstadt within a research project in cooperation with a distribution network operator [34]. Within the past few years, the experimental setup has been constantly modified and optimized. In this paper, the detailed experimental setup, operational experiences, as well as some effects of varying cable operations on different bedding materials are presented.

2. Materials and Methods

2.1. Experimental Setup

The test site is located at the August-Euler-Airport, which is part of TU Darmstadt, in Griesheim near Darmstadt and can be distinguished into two testing areas: a main field with various cable configurations laid in four different bedding materials, and a side field with additional cable trenches for thermal enhanced bedding materials and protection pipe systems (Figure 1). Adjustable high-current transformers provide the electrical load for the cables, a weather station delivers meteorological information, and the changes of the thermal and hydraulic conditions within the test site are monitored by numerous sensor configurations.

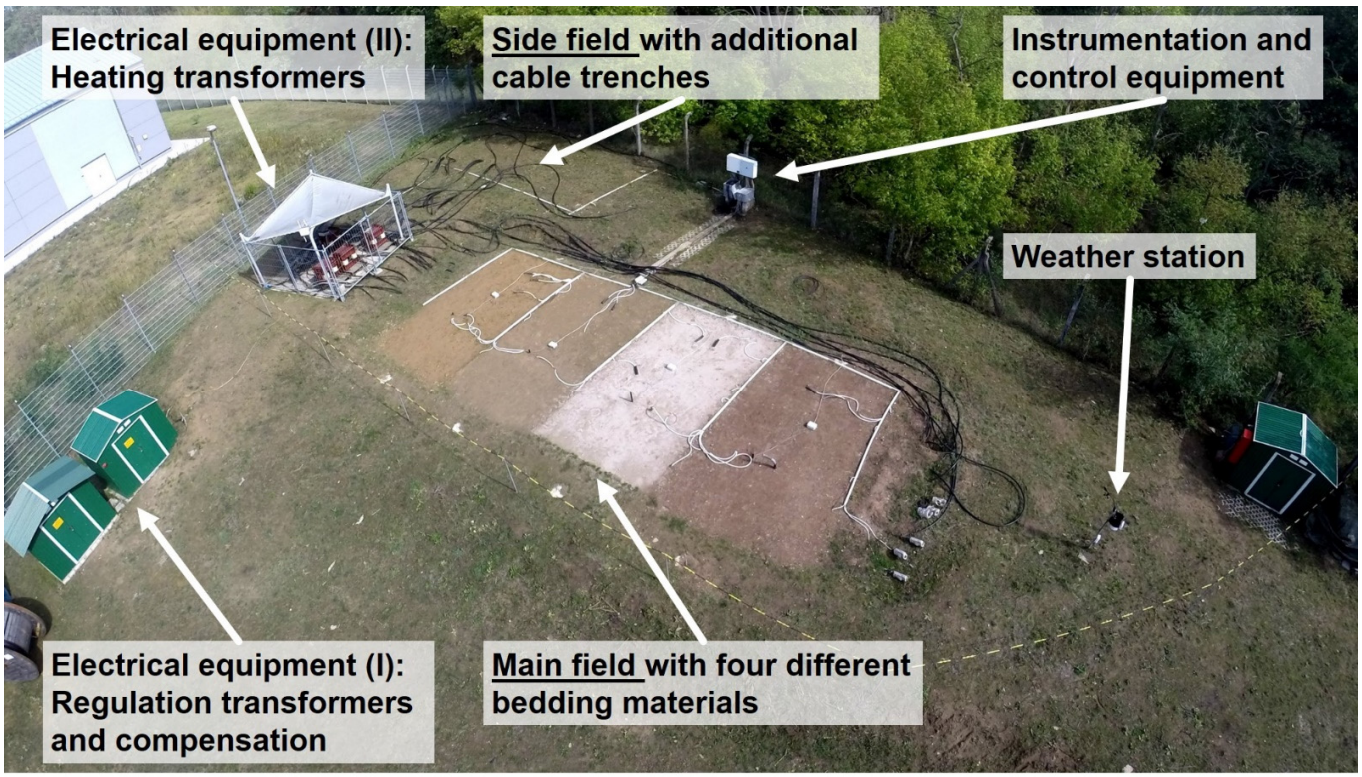

Figure 1. Aerial photograph of the test site with its main and side field as well as the electrical and monitoring equipment.

The natural geological setting of the area at the test site is dominated by a mostly homogenous soil, consisting of Pleistocene drifting sand with a possible anthropogenic influence due to its intensive usage for military and civil purposes since the end of the

19th century [35,36]. The area is located at around 110 m MSL, and continuous measurements of observation wells conducted by a local water supplier in the immediate vicinity of the area reveal that the minimal distance of the ground water table to the surface is about 14 m. Considering that the maximum capillary rise for a fine sand is expected to be of around 1 m, this indicates that there is no capillary connection of the ground water table to the test site due to capillary action. Therefore, it can be presumed that the hydraulic situation within the test site area is only affected by meteorological influences.

Three different cable types, one LV-cable and two different MV-cable types, were used in the various cable configurations within the test site at depths between 0.6 m and 1.0 m. The specifications of the cables used are summarized in Table 1. The selected cable types represent the most commonly used cables in the distribution network of the industrial partner with whom the test field was planned. Corresponding with the real scale practical applications, the LV-cables were laid individually and the MV cables were laid in trefoil configuration. Special care was taken to allow for the direct measurement of the conductor and outer sheath temperatures of the different cable configurations in the various bedding setups. To this end, prior to the cable installation, the respective cable sections were modified using PT100 temperature sensors.

Table 1. Overview of the used power cables and corresponding manufacturer information.

Attribute	Unit	NAY2Y-J SE 4 × 150	NA2XS(F)2Y 1 × 150 RE/25	N2XS(F)2Y 1 × 400 RM/35
No. of cores × nominal cross section	mm^2	4 × 150 SE	1 × 150/25 RE	1 × 400/35 RM
Conductor Material		Aluminum	Aluminum	Copper
Insulation Material		PVC	XLPE	XLPE
Nominal insulation thickness	mm	1.8	5.5	5.5
Nominal sheath thickness	mm	2.5	2.5	2.5
Outer diameter approx.	mm	48	34	44
Rated voltage	kV	0.6/1	12/20	12/20
DC resistance at 20 °C	$\Omega\ km^{-1}$	0.206	0.206	0.047
Capacitance	$\mu F\ km^{-1}$	n. a.	0.24	0.358
Max. operating conductor temperature	°C	70	90	90
Used in configurations	Main field	I, II, III	II, III, IV	
	Side field		V, VI, VIII, IX, X	VII

2.1.1. Main Field

The overall dimension of the main field is 14 × 6 m. It is divided into four sections, each of 3.5 m length that are hydraulically and thermally decoupled from each other by impermeable plastic layers and 20 mm thick Styrofoam plates. To represent the variety of possible bedding materials for directly buried cables, the naturally occurring sand on the site was replaced by silt and loam in two of the four sections up to a depth of 2.5 m. In one section the naturally occurring sand was maintained and in another section the cables were laid on the sand and subsequently backfilled with a commonly used artificial fluidized backfill material up to ground level. Fluidized backfill materials are used in cases where consolidation work should not be applied, and where a volume-stable backfilling is required. This includes, for example, crossings of multiple infrastructure lines in urban areas. Figure 2 presents a sketch of the main field with the four different cable configurations in the four bedding materials. During the construction of the field test, targeted efforts were made to ensure that the cables could be spatially allocated as accurately as possible. For this purpose, the cable laying level was first established, then the cables were positioned and comprehensively geodetically surveyed, before they were subsequently backfilled with the corresponding bedding materials to its current surface. To avoid any difficulties caused by the hydraulic interaction with plant roots, any vegetation was regularly removed from the ground level.

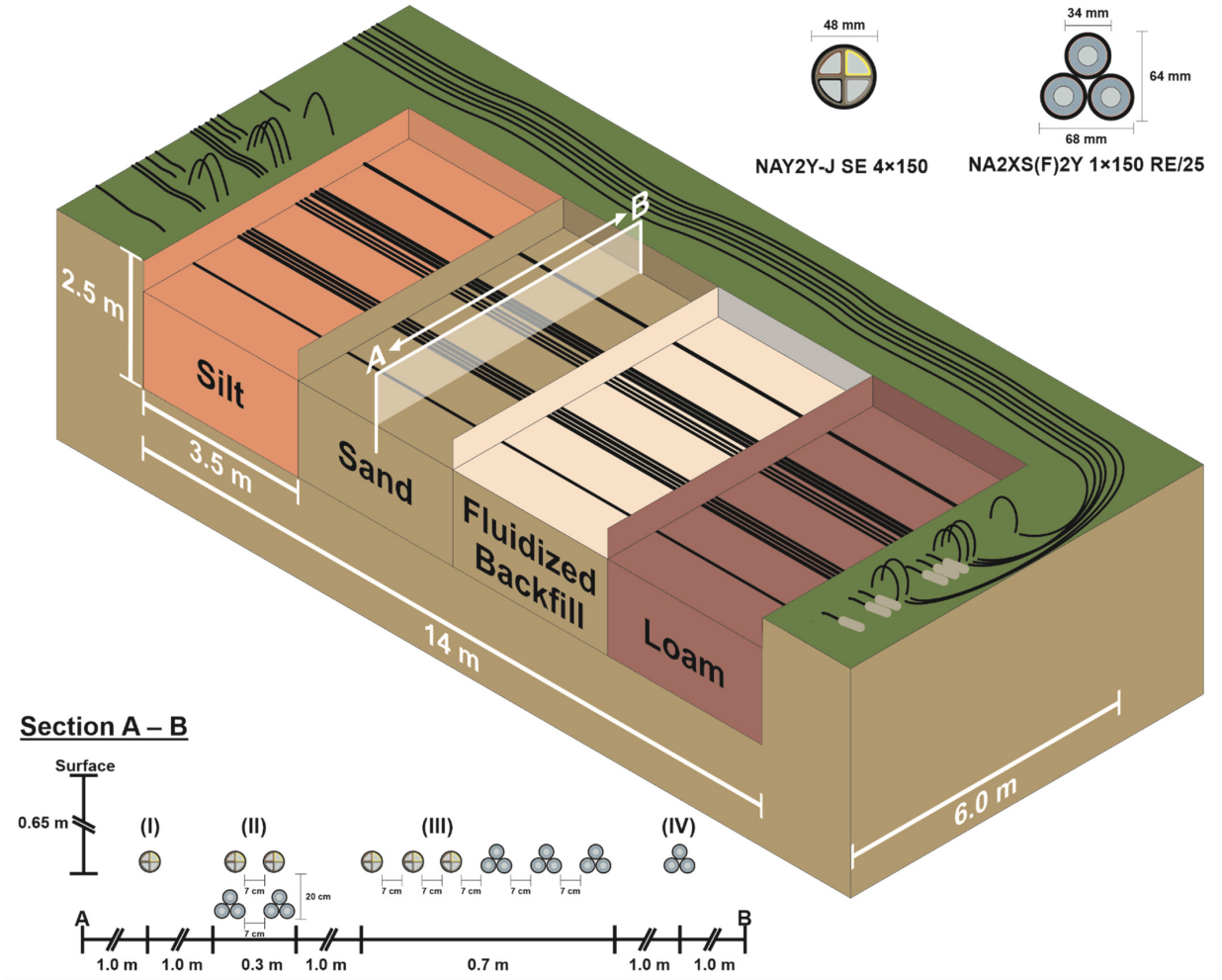

Figure 2. Sketch of the main field of the test site, showing the four different cable configurations (roman numerals) in the section A-B: (I) Single LV-Cable; (II) Two LV-Cables with two MV-Trefoils; (III) Three LV-Cables and three MV-Trefoils arranged in a row; (IV) Single MV-Trefoil.

Four different cable configurations of LV-cables (NAY2Y-J SE 4 × 150) and MV-cable-trefoils (type NA2XS(F)2Y 1 × 150 RE/25) have been embedded in the field at depths between 0.65 m and 0.85 m according to the German standard [37]. The single configurations of the LV cable and the MV (trefoil) cables (Figure 2, I and IV) allow for the investigations on the changes of the thermal and hydraulic properties in the surrounding of only one cable setup. Cable configurations II and III, represent the cable configurations of common cable trenches and can be loaded in different scenarios to investigate their mutual influence between and within their surroundings.

The bedding materials used were selected to represent a maximum variance of soil types. The three natural soils can be classified as silt loam, sand, and loam according to the USDA soil texture triangle. However, alongside grain size distribution, other geotechnical and hydraulic properties of the soils were also taken into account. The geotechnical properties of the used bedding materials are listed in Table 2. The hydraulic and thermal properties, shown in Figure 3, of the materials were measured using a modified evaporation test, as described in [38], to measure the relevant hydraulic and thermophysical properties of a soil or bedding material sample simultaneously. To increase the accuracy of the water retention characteristics in the dry range (pF > 4), complementary data points were obtained with a WP4C dew point potentiometer.

Table 2. Geotechnical properties of the bedding materials in the main field.

Property	Unit	Silt	Sand	Fluidized Backfill	Loam
D_{10}	mm	0.007	0.09	0.18 *	<0.001
D_{30}	mm	0.02	0.14	0.34 *	0.006
D_{50}	mm	0.03	0.19	0.51 *	0.04
D_{60}	mm	0.04	0.21	0.63 *	0.06
Uniformity coefficient C_U	-	5.7	2.3	3.5 *	>15
Bulk Density	$g \cdot cm^{-3}$	1.72	1.62	1.64	1.75
Grain Density	$g \cdot cm^{-3}$	2.67	2.66	2.75	2.75
Porosity	%	35.6	39.1	40.4	36.4
Organic Content	M.-%	1.9	1.1	0.8	1.4

* Dry raw materials prior to hardening.

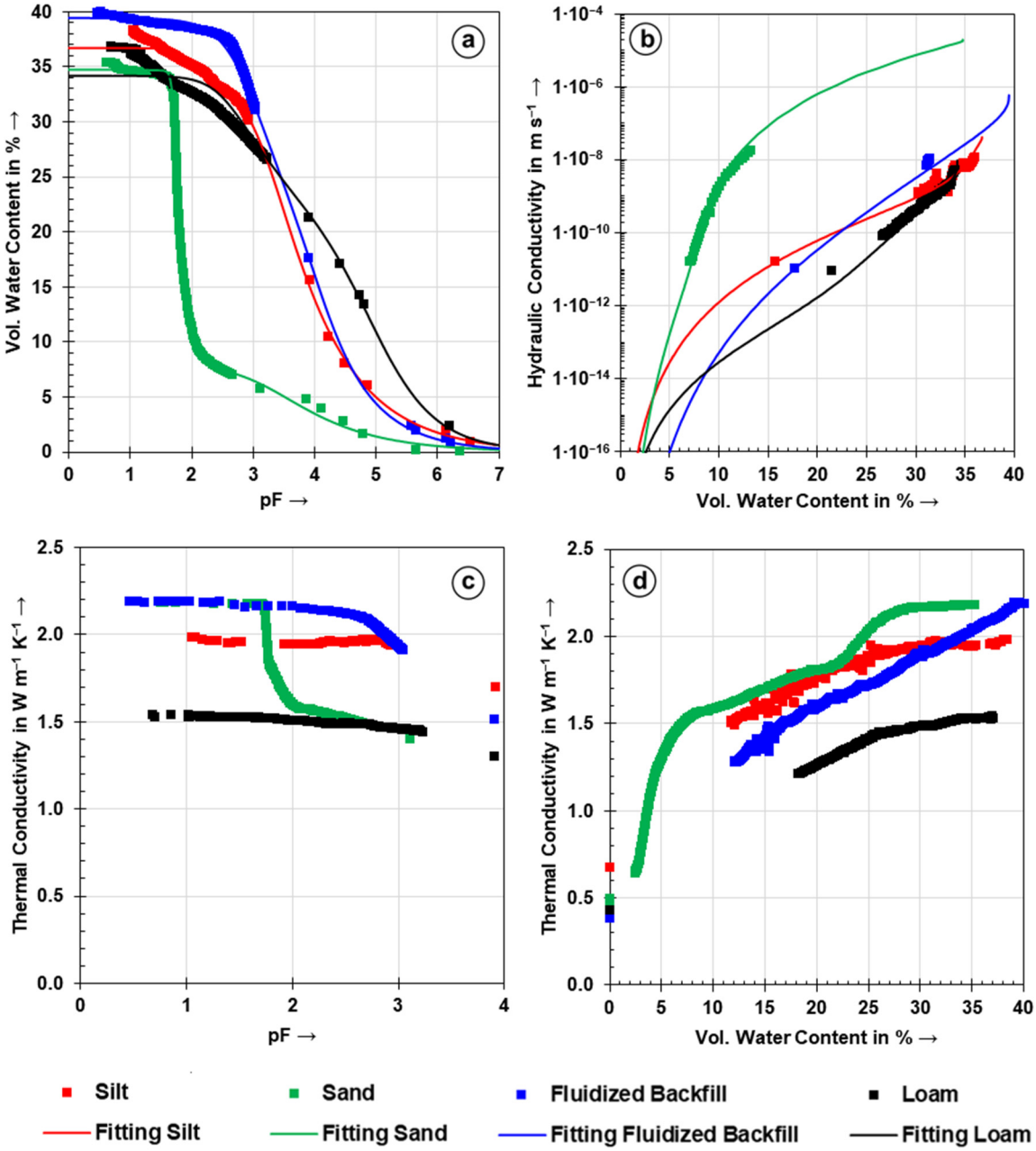

Figure 3. Overview of the important hydraulic and thermal properties of the bedding materials of the main field: Water retention characteristics (**a**), unsaturated hydraulic conductivity characteristic (**b**), thermal conductivity as a function of the hydraulic potential (**c**), thermal conductivity dryout curve (**d**).

2.1.2. Side Field

Besides the main field, several additional cable configurations have been installed in the side field (Figure 4). On the one hand, two MV-Cables (NA2XS(F)2Y 1x150 RE/25) in a trefoil configuration, were placed in PVC-ducts with an inner diameter of 147.6 mm and a wall thickness of 4.8 mm to perform an investigation of the heat dissipation processes in protection pipe systems. Cable ducts are often used to temporarily decouple constructional works from the corresponding cable laying measures or for an additional mechanical protection of the cables. In the side field, the ducts have been buried in the natural sandy soil at a depth of 0.75 m (lower outer edge duct—ground surface). One of the protection pipe systems has been left air-filled while the other was filled with a special artificial thermal enhanced grouting material with a thermal conductivity of around 2.5 W m^{-1} K^{-1}.

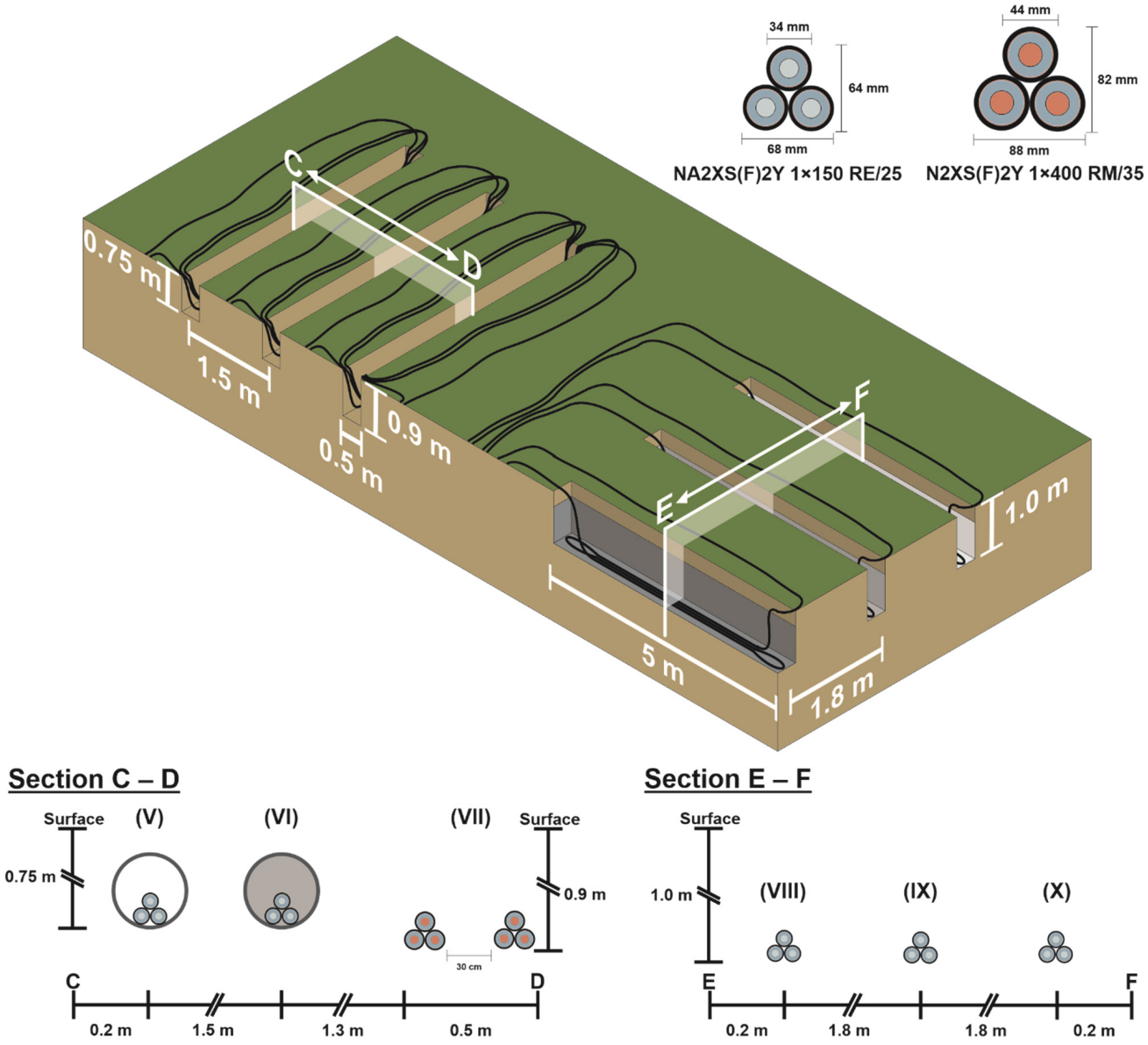

Figure 4. Sketch of side field with six additional cable trenches. Cable configurations in section C-D are: (V) Single MV-Trefoil in unfilled protection pipe; (VI) Single MV-Trefoil in protection pipe filled with artificial grouting material; (VII) Two copper MV-Trefoils. Cable configurations in section E–F are: (VIII) Single MV-Trefoil in artificial bedding material with high thermal conductivity; (IX) Single MV-Trefoil in artificial fluidized backfill material with high thermal conductivity; (X) Single MV-Trefoil in artificial grouting material with low thermal conductivity.

On the other hand, three additional cable trenches have been constructed for a comparison of three artificial bedding materials. One MV-Cable trefoil-configuration (NA2XS(F)2Y 1 × 150 RE/25) was bedded at the bottom of each trench.

Two additional MV-Cable-trefoil configurations (N2XS(F)2Y 1 × 400 RM/35) have been embedded directly into the natural sandy soil at a depth of 0.9 m at some distance from the main field for an investigation on heating cables with higher conductor cross sections of 400 mm^2.

2.1.3. Electrical Equipment and Cable Operation

To provide the electrical load for the cables, high-current transformers that are supplied by adjustable transformers, are used to inductive couple the test current in the cables (Figure 5). The adjustable transformers are automatically regulated by a microcontroller with a peripheral circuitry for measuring, controlling, and communication via TCP/IP. In combination with the measured cable-temperatures (conductor/sheath) and the actual load on the cables via AC/DC current transducers (AHR 500 B10—Current Sensor with true RMS value, accuracy = 1%), this system allows for the heating of the cables to the critical values as well as for applying any dynamic load profile on the cables.

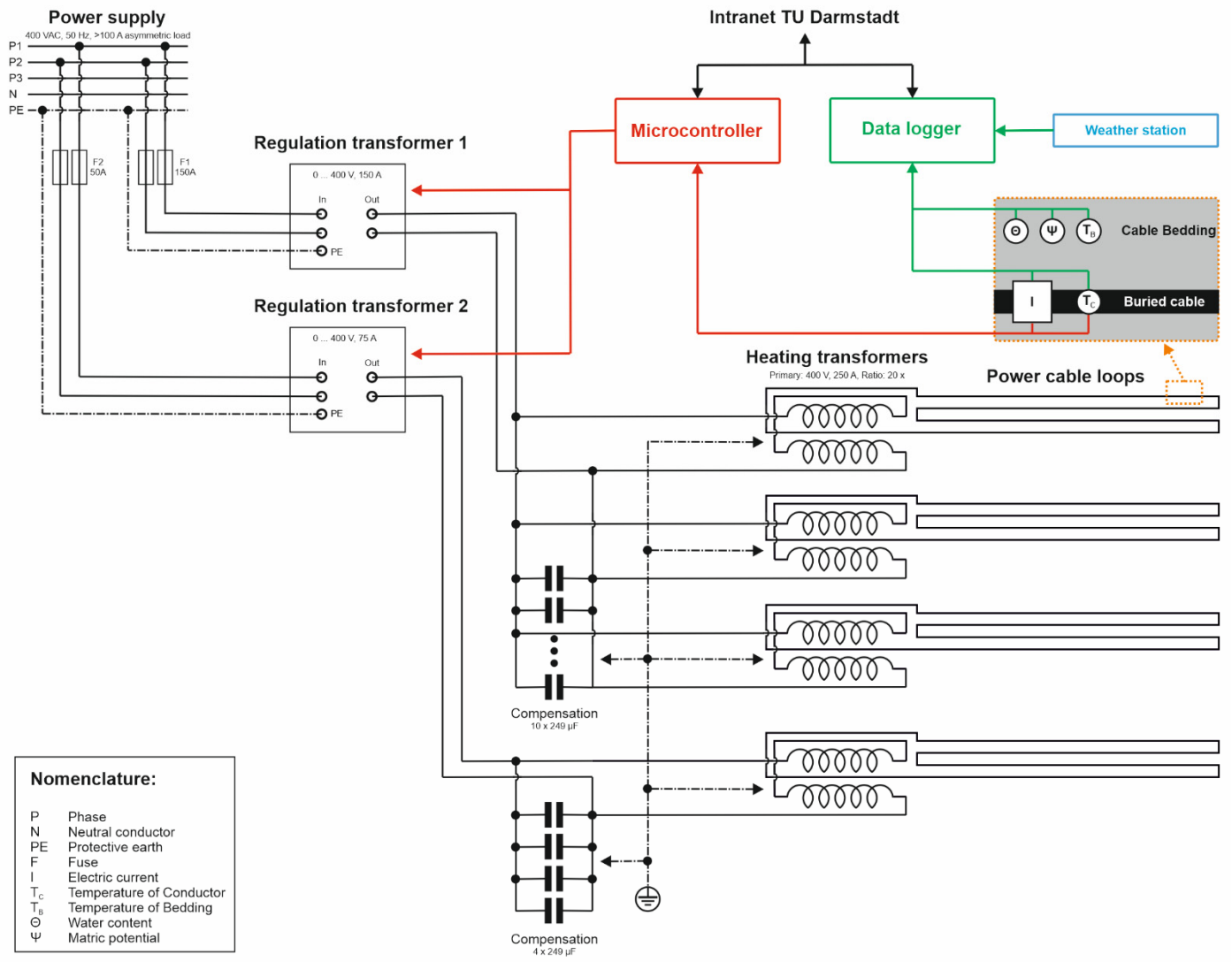

Figure 5. Concept of providing the electrical load and operation of the test site.

Although the intention was to construct an experimental setup that permits the investigation of the cable heating processes as realistically as possible, some restrictions had to be made due to constructional and technical limitations.

The thermal losses of a cable system consist mainly of resistive conductor losses. These losses are in a quadratic relationship to the conductor current and remain independent of the applied voltage. In the experimental setup, currents in the same range as the current used for real cables are applied, however, at notably lower voltages (<20 V). Because of the single phase induction presented in Figure 5, the cables are operated using an open screen and are not charged by a symmetrical three-phase current. The resultant differences in the cable losses with respect to operational conditions have been considered. For this purpose, analytical calculations of the losses were made according to [10]. The corresponding results for the used 150 mm^2 and 400 mm^2 MV-cables are represented in Table 3. In addition to the screen losses of the copper cable, the losses of the cable systems are represented at the test site configurations in a reasonable way.

Table 3. Comparison of calculated losses of 150 mm^2 aluminum (NA2XS(F)2Y 1 × 150 RE/25) and 400 mm^2 copper (N2XS(F)2Y 1 × 400 RM/35) MV cables at maximum operating temperatures.

Place of Loss	Type	Percentage of Overall Losses		Occurrence at TU Darmstadt Test Site
		150 mm^2	400 mm^2	
Conductor	Resistive Losses	97.02	81.86	Yes
	Losses due to Skin Effect	0.22	5.12	Yes
	Losses due to Proximity Effect	0.11	2.09	Negligible differences due to phase position
Dielectric	Dielectric Losses	0.05	0.05	No
Screen	Resistive Losses	2.60	10.88	No

In contrast to real-world applications, where usually only three conductors are loaded, the LV-cables used in the test site are loaded by all four conductors, including the PEN conductor to reduce the required effort and the possible additional thermal influences through an additional looping of the cables above the surface. In order to take this into account, the load is adjusted using conversion factors that are derived from numerical electro-thermal simulations. The prerequisite of the investigation was to obtain the same maximum conductor temperatures for loadings in the test site as in the case of loading in the regular distribution network. This could be ensured by a corresponding characteristic curve for the LV-cables, stored in the microcontroller of the test site.

Due to the limited size of the test site, the length of the cables within each of the different bedding materials is also limited. To minimize any potential boundary effects, the four sections are thermally decoupled from each other using Styrofoam plates and all the measurements are obtained from the middle of the respective bedding fields. However, the longitudinal thermal flux along the conductor, consisting of high thermal conductive materials such as copper or aluminum, cannot be prevented using this method. Numerical simulations showed that the mutual thermal influence at the bedding interfaces can occur for up to a few meters; particularly for two bedding materials with significant differences in their thermal conductivity. Additionally, due to constructional restrictions, the cables must form closed loops and lead back above the surface. This results in additional and different heat dissipation processes along the cables and might also influence the bedding sections at the ends of the test site. For the test site configurations, numerical simulations revealed that the influence on measured data in the area of the sensors, located in the middle of the different bedding sections, are negligibly low.

2.1.4. Monitoring Strategy and Equipment

The changes of the thermal and hydraulic conditions that have natural and operational causes within the test site are monitored by numerous sensors. 80 Pt100 resistance thermometers (accuracy class 1/10 DIN B according to DIN EN 60751) are installed at

the cable conductor and the sheath, as well as the surrounding bedding material to capture a detailed image of the temperature distribution within the test site. Furthermore, 15 Frequency-Domain-Reflectometry (FDR) sensors (METER Group, ECH$_2$O EC-5, accuracy = ±3% volumetric water content) measure the volumetric water content of the bedding material and 16 tensiometers (METER Group, T4e, accuracy = ±5 hPa) are used to measure the matric potential in the bedding to detail the moisture movements.

Additionally, fiber optic cable loops were installed in the main field in depths of 1.3 m and 2.5 m to allow for a detailed spatially resolved planar temperature measurement with the Distributed-Temperature-Sensing (DTS) method. However, the spatial temperature differences occurring at such a distance to the cables do not prove to be significantly higher than the uncertainty of the DTS measurement method. Nevertheless, the measurements can be used to derive the planar temperature date for the level beneath which the cables have been laid.

Besides the permanent installed sensors, additional sensors were installed temporarily depending on the loaded cable configurations. For this purpose, four temperature sensors (PT100) were mounted in notches along fiberglass rods of 1 m length (Ø = 40 mm) in several predefined positions to allow for flexible temperature measurements in defined distances to the heated cables.

2.2. Load Profiles

2.2.1. Constant Scenario

The simplest case was just applying constant load (m = 1), or rather increase the constant load stepwise when a steady temperature distribution could be assumed, whereby the load factor m is defined as the daily integral load divided by the peak load. For constant load measurements, two methods could be used: the load was either maintained as a constant or the criteria for the automatic regulation of the adjustable transformers were defined based on the actual measurements of one special or several relevant temperature sensors. Such methods allow for a cable loading in accordance with the maximum operating (conductor) temperatures.

2.2.2. Dynamic Scenario

One major purpose of the construction of the test site was to investigate and quantify the potential load capacity reserves in distribution grids against the background of changing load profiles resultant of an increase in the volatile energy production. Hence, one important task was to identify adequate load profiles as well as to allow for an application of the dynamic load profiles on the cables within the test site.

A standard daily load profile (SLP) was used to represent the former and still partially present load case in distribution grids. For this purpose, the commonly used "EVU-Profile" (m = 0.7), as represented in Figure 6, was implemented in the automatic load regulation of the test site. The EVU load profile represents an average daily load cycle, composed of the average shares of consumers from different households and industries in a grid with a centralized energy supply. An increased amount of decentralized renewable energy might significantly change the shape of such a daily load profile.

To represent the increasing proportion of volatile energy production, a load profile (PV-profile) (m = 0.4) was developed based on real measurements of a MV transformation station located in an area with a proportion of installed photovoltaic capacity (about 3.5 kWp per household), much higher than the German average. Hence, this load profile can be considered as a future common loading scenario in context to Germany's energy transition. With the inevitable load peaks it is also a worst-case scenario for current rating of buried electric cables. The used daily load profile is based on the measurements of a working day, outside of holiday seasons and without unusual sunny weather. The ratio of the load peak at noon to load during the night is around 5:1, and therefore comparable to the data of other time periods. Further relevant details include the use of a constant load level during the night, the reduction of the residual load with increasing insolation, during

noon similarities with a pure PV load profile and a slight increase of the load occurred after sunset.

For the test site, the measured load data had to be adapted because in case of only transferring the measured current value, the actual zero crossing (change in direction of power transfer) would not be accounted for. Therefore, the apparent power (appropriately signed) was used to load the test site cables.

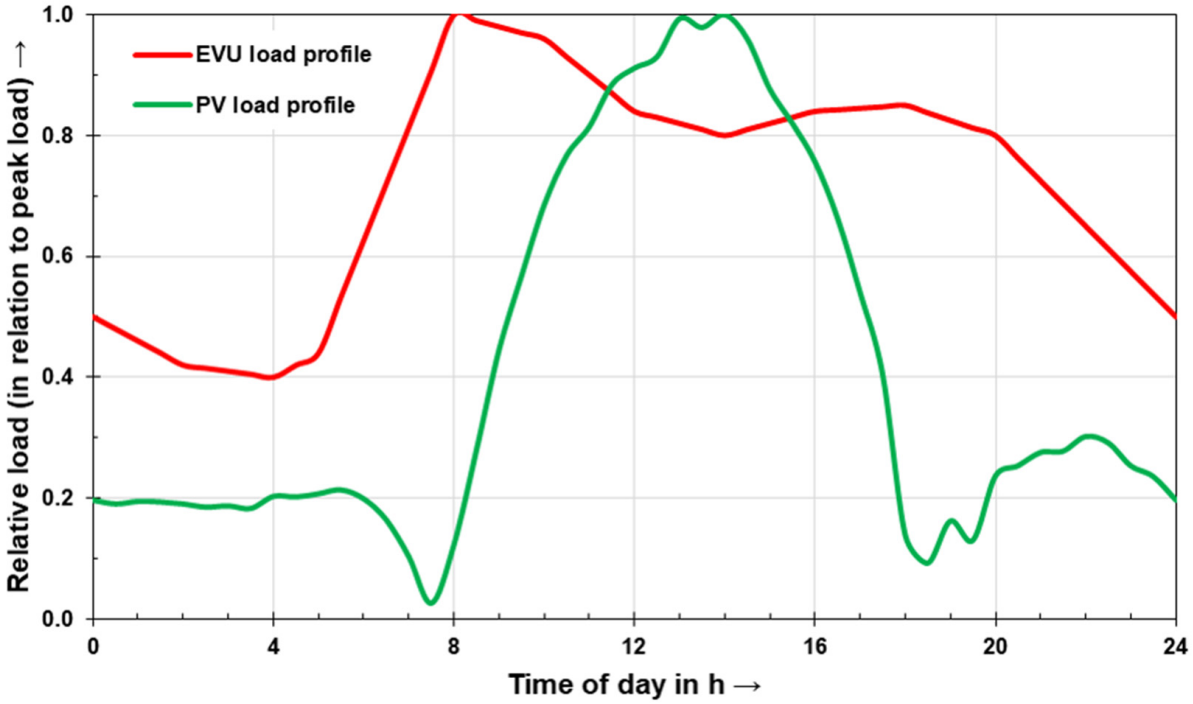

Figure 6. Load profiles to represent the dynamic loading of buried cable configurations.

3. Results

3.1. Constant and Dynamic Loading of Single MV-Trefoil (IV)

During a long-term test, the single MV-Trefoil configuration of the main field (IV) was subjected to electrical load over a period of around nine months. For this purpose, electric power was initially applied at a continuous load (m = 1) for four months, followed by five months with different dynamic load profiles. Exemplary results of this experiment are presented in Figures 7 and 8.

Figure 7 shows the measured conductor temperatures within the four different bedding materials, the electrical load, and the weather station data of the last 5.5 weeks of the constant loading experiment. Until the displayed time series, the cable assembly had already been constantly loaded with the maximum load, specified by the cable manufacturer, at about 319 A for several weeks. As indicated by the conductor temperatures, the influence of the effective thermal conductivity properties of the different bedding materials becomes evident. While temperatures above 80 °C were consistently reached in the loam, the conductor temperatures in the other beddings were generally significantly lower. Furthermore, from around day 35, a significant reduction in the conductor temperature was observed in the sand bedding. This is due to intense rainfall after a prolonged dry weather period, causing a gradual rewetting in the sand bedding and thus improving its heat conduction properties. This illustrates the influence of the different hydraulic properties (especially hydraulic conductivity) of the various bedding materials. Thus, only the sand shows a strongly dynamic reaction to changing weather conditions.

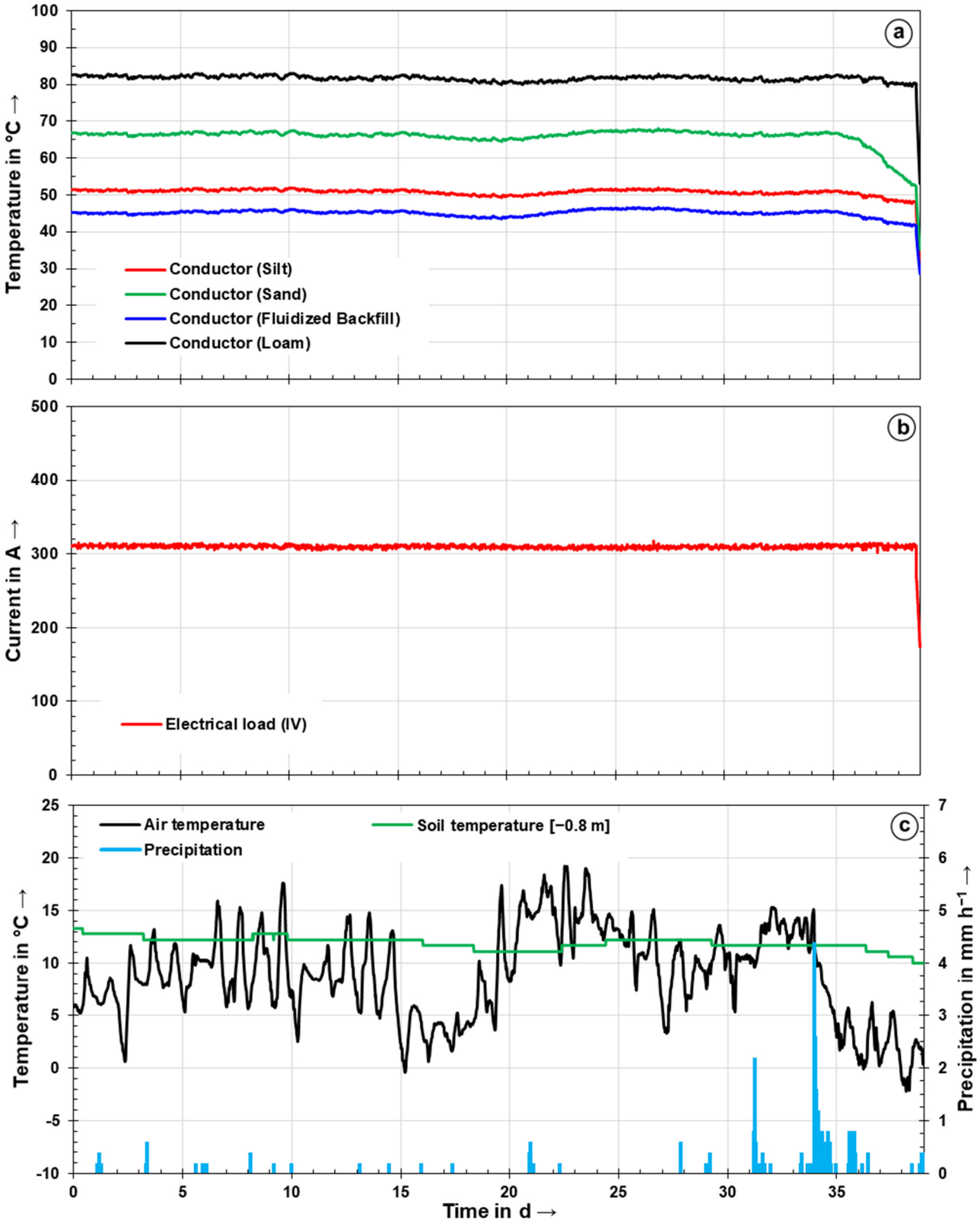

Figure 7. Measured temperatures (**a**), electrical load (**b**), and weather station data (**c**) of the constant loading experiment of the single MV-trefoil (IV).

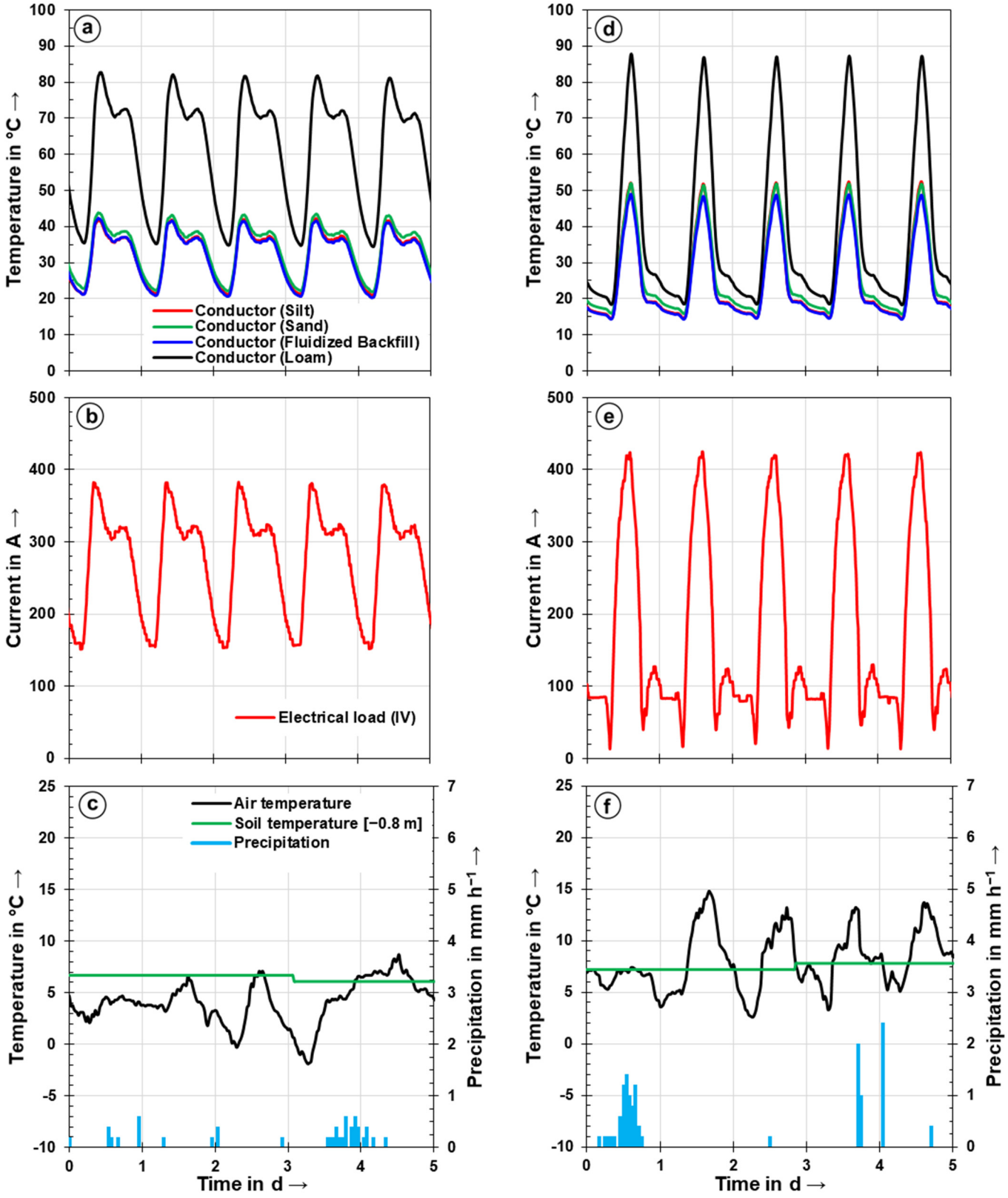

Figure 8. Measured temperatures (**a**,**d**), electrical load (**b**,**e**), and weather station data (**c**,**f**) of the dynamic loading experiment with the EVU-profile (left; **a**–**c**) and the PV-profile (right; **d**–**f**) of the single MV-trefoil (IV).

Figure 8 shows the measured conductor temperatures within the four different bedding materials, the electrical load, and the weather station data, applicable for all three weeks of the dynamic loading experiments with the EVU-profile and the PV load-profile, re-

spectively. For both experiments, the load was selected in order to represent the respective permissible peak loads according to IEC 60853 (thermal resistivity of soil = 1.0 K m W^{-1}; ambient temperature = 20 °C; no drying-out). Again, the loam shows by far the highest conductor temperatures with peak temperatures above 80 °C in both cases, illustrating the load-limiting influence of bedding materials with comparatively low apparent thermal conductivity across an entire cable route.

3.2. Constant and Dynamic Loading of Ducted Systems (V + VI)

Placing a cable in an air filled (unfilled) duct usually leads to an increased thermal resistance between the cable surface and the substrate surrounding the ducts. For the same electrical load, this might result in an increased temperature of the cable located in the duct compared to a directly buried cable. To investigate the thermal performance of a ducted system, both a cable configuration (V) with a single MV-trefoil in an unfilled duct and a configuration (VI) with a single MV-trefoil in a protection pipe filled with artificial grouting material were simultaneously subjected to constant and dynamic loading for approximately eight weeks during the winter season. Both cable systems were loaded using one of the two regulation transformers, allowing simultaneous power supply even in the case of different loads.

Figure 9 shows the measured conductor temperatures as well as the temperatures at the outer surface of the duct, the applied electrical load, and the weather station data of the 33 days of the constant loading experiment. During the first 18 days, both systems were subjected to an electrical load of 300 A, which was the ampacity of the unfilled ducted system according to IEC 60287 (thermal resistivity of soil = 1.0 K m W^{-1}; ambient temperature = 5 °C; no drying-out). The loading of the ducted systems resulted in higher temperatures in the unfilled protection pipe system, compared to the grouted protection pipe system. Following this, the load control system was adjusted so that the same conductor temperatures of around 90 °C were achieved in both systems. Through an analysis of the data, an increase in the ampacity of up to 25% could be monitored for the grouted system (VI), compared to the air-filled protection pipe system (V).

Figure 10 illustrates the same measured parameters for the dynamic loading experiment with a daily repetition of the EVU-profiles, directly following the constant loading experiments. Initially, a peak load of 320 A for the unfilled ducted system was applied as this comprised the ampacity of this system according to IEC 60853 (thermal resistivity of soil = 1.0 K m W^{-1}; ambient temperature = 5 °C; no drying-out). The load of the grouted duct was selected, so that similar conductor temperatures in both ducted systems were achieved. During the experiment, the electrical load was increased twice to approach conductor temperatures in the range of the permissible 90 °C. Again, it was possible to load the grouted duct system at a considerably higher level than for the unfilled system, allowing for an increase in the peak load of around 35%. Furthermore, it can be noticed that the first load peak of the EVU-profile leads to a less apparent increase of the conductor temperature in the grouted pipe system and appears as rather damped. This effect is primarily caused by the higher heat capacity of the artificial grouting material compared to the air in the unfilled protection pipe.

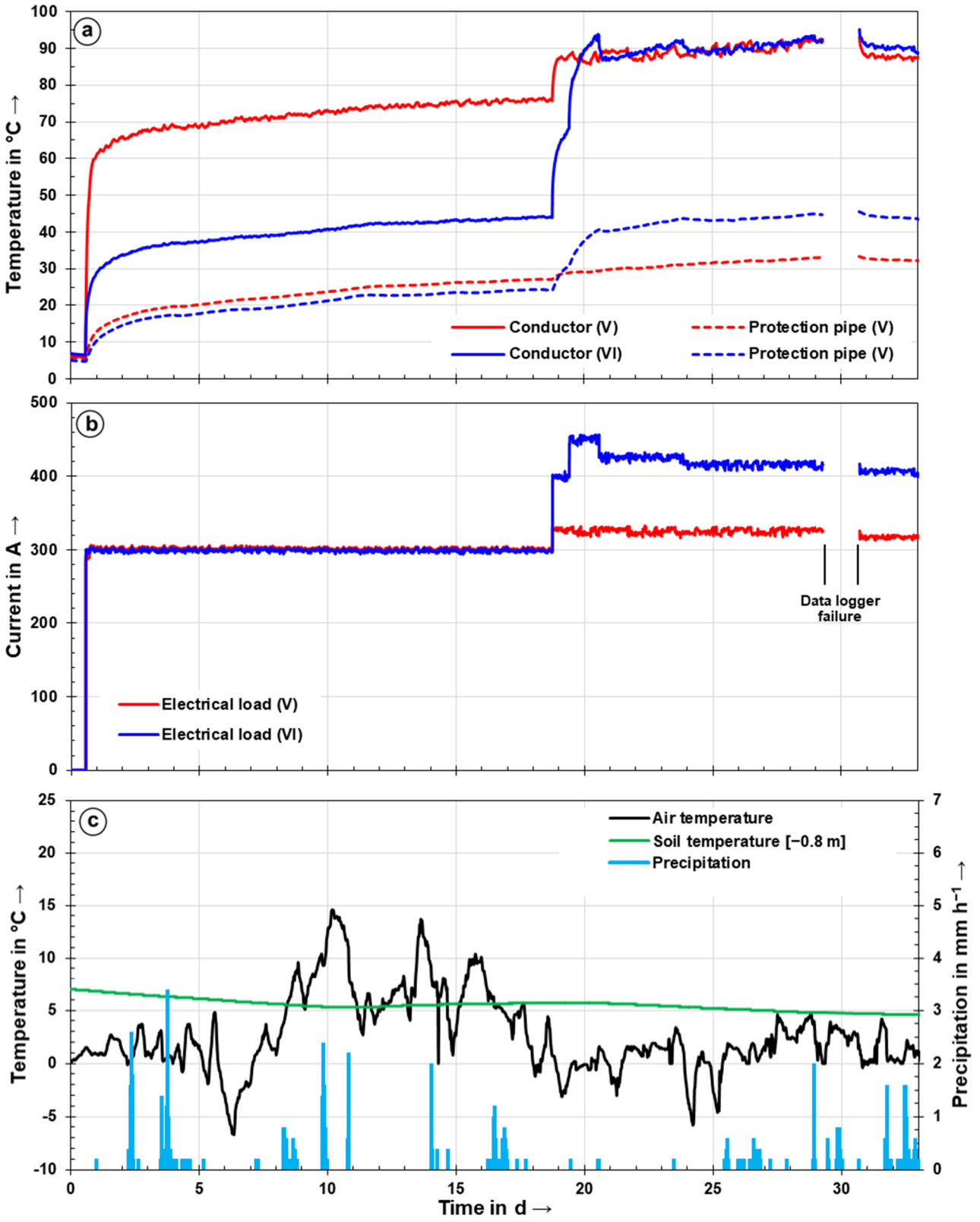

Figure 9. Measured temperatures (**a**), electrical load (**b**), and weather station data (**c**) of the constant loading experiment of the protection pipe systems (V) and (VI).

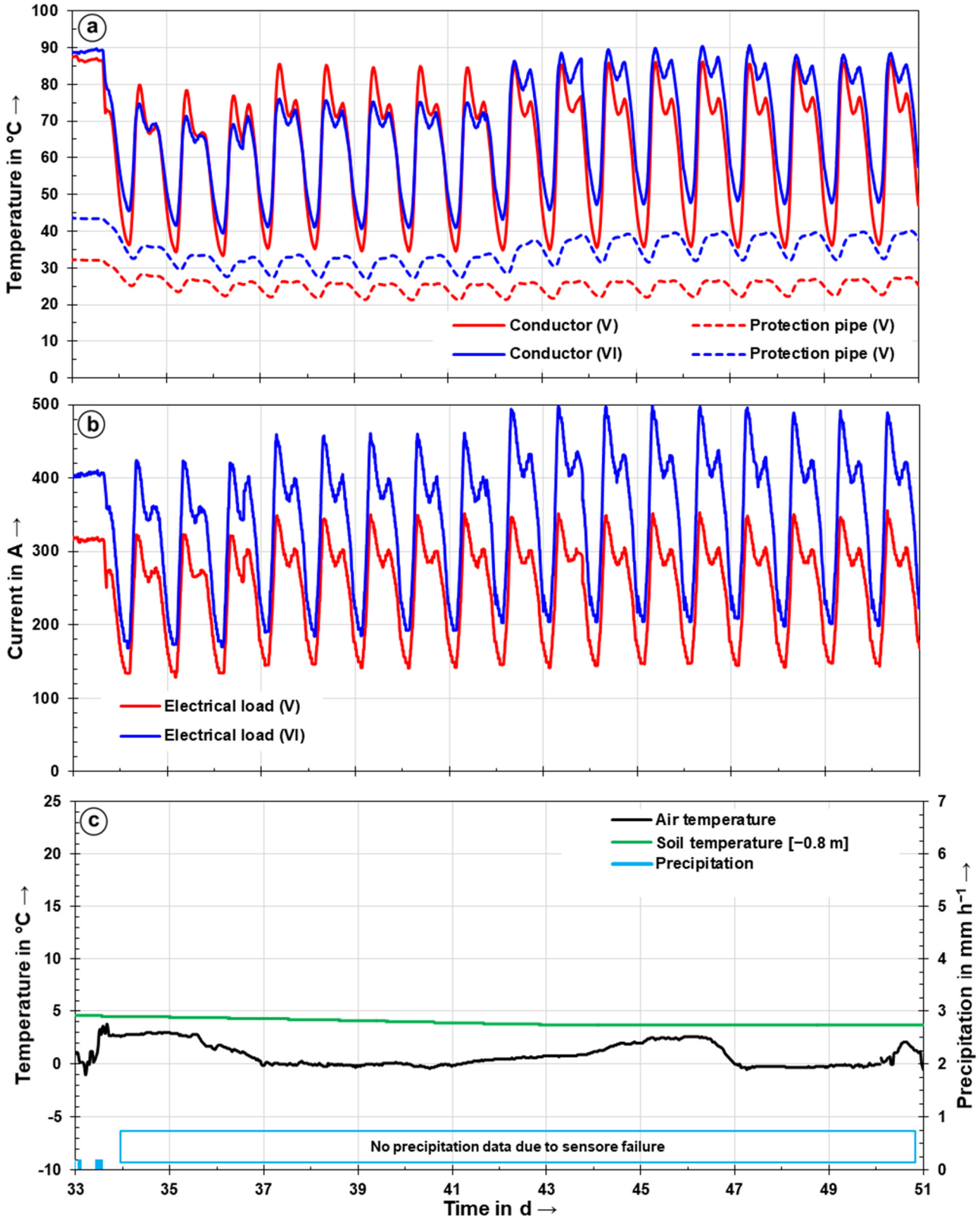

Figure 10. Measured temperatures (**a**), electrical load (**b**), and weather station data (**c**) of the dynamic loading experiment of the protection pipe systems (V) and (VI).

3.3. Effect of Drying-Out and Rewetting during Long Term Experiment of Double MV-Trefoils (II)

During a long-term test, the two MV-Trefoils of configuration (II) within the main field were subjected to an electrical load over a period of about eleven months. For this purpose, the electric power was initially applied at a continuous load for four months, followed by five months with different dynamic load profiles and two further months of a continuous load.

Figure 11 shows the measured sheath temperatures, the electrical load, water content, and the weather station data of the last five weeks of the final constant loading experiment. In contrast to the results from the configurations previously presented, the measurement data of temperature sensors directly attached to the conductor were not available for all beddings of the two MV-Trefoils in configuration (II). Thus, the available data of sensors attached at the cable sheaths were used as temperature information. The FDR-sensors for the water content measurements affected by the experiment were placed at a slightly elevated level between the two MV-Trefoils at a distance of approximately 10 cm to the cable trefoils. The undisturbed water content was measured at a horizontal distance of at least 2.5 m and for the same depth as configuration (II) in the bedding sections between configurations (III) and (IV).

Initially, the constant load was applied at 280 A and the highest cable temperatures were measured again in the loam bedding. The other beddings presented a significantly lower temperature level. Towards the end of the first week, an increase in measured sheath temperatures occurred in all beddings as a result of the warm weather. As a consequence, the temperature limit value of 75 °C for the sheath temperature was reached in the loam, which led to scattering that can be seen in the measured values due to the corresponding automatic control of the actual electric load. This is why the load was later reduced to 260 A, which resulted in almost constant temperatures in the cables as the test progressed. An exception to this was the sand bedding, which continued to experience a steady rise in cable temperature. From around day 27, the temperatures of the loam were also exceeded and the temperature limit of 75 °C for the sheath temperature was reached. By studying the measured water content values, it is clear that this effect was related to partial drying around the cables in the sand bedding. As a result of the relatively dry weather with only occasional levels of low precipitation over several weeks, there was also a slight reduction of the water content in the areas unaffected by the cable operation. However, the reduction in water content in these areas was comparatively low, whereas in the vicinity of the cables in the sand, complete drying occurred from around day 14. In this context, the different drying behaviors of the various beddings becomes evident. Although a slight reduction of the water content occurred in the loam and somewhat more clearly in the silt, a complete drying-out as in the sand was not reached by any means. The effect of these water content changes on the cable ampacity caused by reducing the beddings effective heat dissipation properties can be explained simply by the bedding characteristics presented in Figure 3. The thermal conductivity of the sand is around 1.7 W m^{-1} K^{-1} at a water content of 11 Vol.-%, while that of the dry sand is 0.5 W m^{-1} K^{-1}. The thermal conductivity of the loam is 1.5 W m^{-1} K^{-1} at a water content of 29 Vol.-%. As the soil area around the cable in the sand dried out, the initially higher apparent thermal conductivity of the sand was reduced to below that of the loam. This resulted in an increased temperature of the cable in the area of the sand bedding. A series of heavy rainfall events with nearly 50 mm of precipitation within 48 h interrupts the drying from around day 28. This led to a rewetting of the bedding materials and thus in the sand in just over one day, and to an almost complete regeneration of the measured values.

In this case study, it is also interesting to note the differences in the temporal duration of the drying and rewetting effects in the vicinity of buried cables. Although the continuous partial drying in the sand occurred over a period of several weeks, the rewetting occurred within a few days.

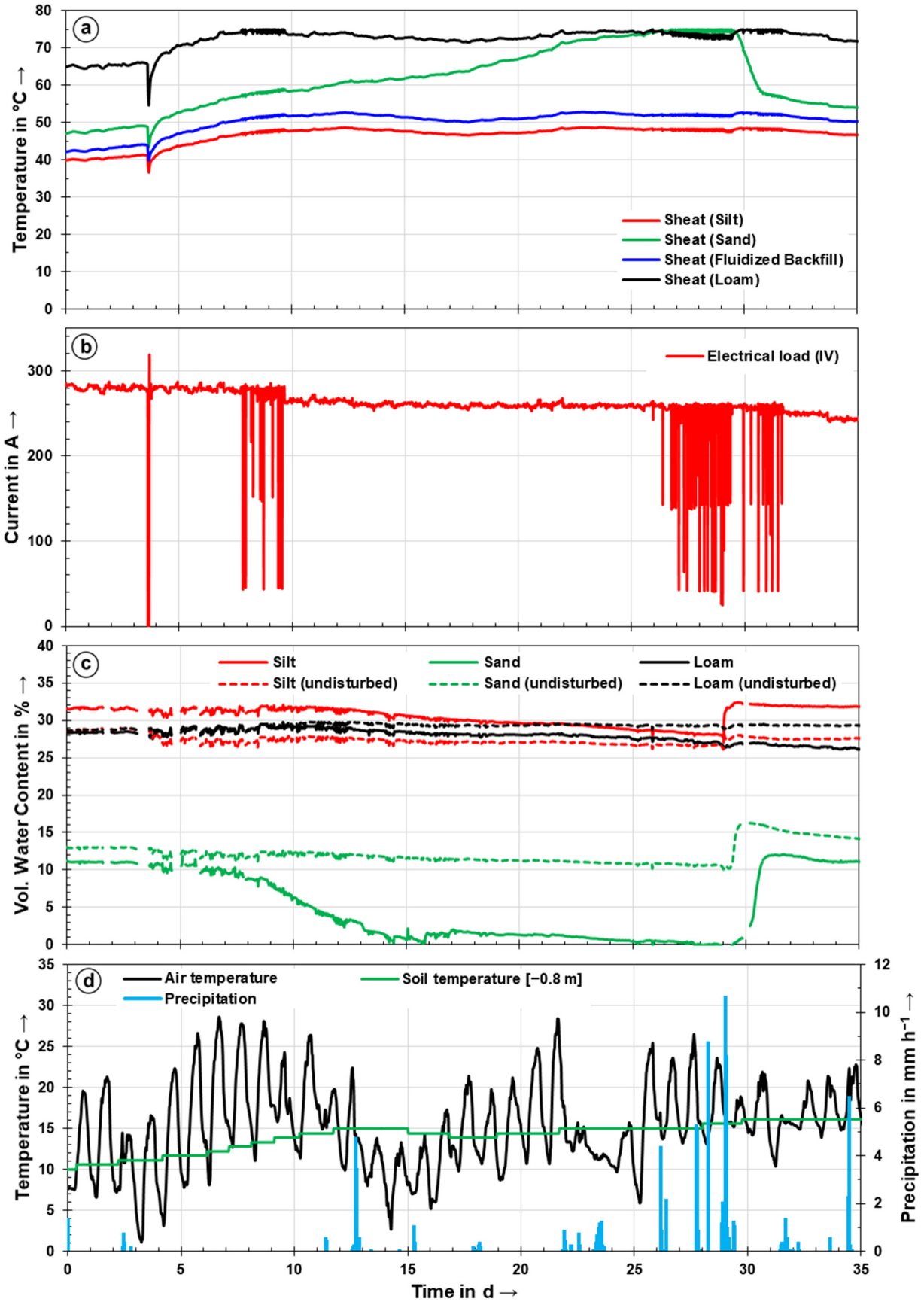

Figure 11. Measured temperatures (**a**), electrical load (**b**), soil moisture (**c**), and weather station data (**d**) during the long-term experiment of the two MV-Trefoils (II).

4. Discussion

4.1. Setup and Operation of a Field Experiment to Investigate Cable Beddings

During the process of planning, construction, and operation of the presented test site, various experiences have been documented with respect to how the real conditions of buried power cables might be simulated accurately in a field experiment and the specific actions that need to be performed so as to achieve this aim. In addition to the basic electrical equipment, this is particularly true for the use of real cables as a heat source as well as the need for appropriate measuring equipment.

Even though the technical effort is greater when using real cables in comparison to the use of equipment such as heated tubes, this additional work should be carried out for investigations in the context of heat dissipation of underground cables to obtain a satisfactory transferability of the results. Although corrections of the directly measured currents may be required depending on the cable loading approach, it can be confidently assumed that the heating of the cables is uniform and corresponds to the real case. For alternative heating systems, additional attention would also be required for the temperature sensing technology involved, especially to prove that the heating on the outside of the heat exchanger is comparable to that of a cable. This applies in particular to dynamic loads, which in fact correspond most closely to the real load conditions in the electrical grid. Furthermore, it appears that investigation results are more likely to be accepted if real cables were used on an accurately representative scale in the conducted experiments, particularly in controversial public discussions, such as those taking place in Germany in the context of the current grid expansions..

Furthermore, the preferable use of real cables is associated with some special characteristics that should be considered in the detailed design of different cable configurations. Since the metallic conductors of the cables have a high thermal conductivity, significant heat conduction can occur along the cable. This has to be taken into account during planning, especially when installing a cable configuration in several different bedding materials or in cases of a return of the cable loop above ground. In addition, when laying a cable configuration in different bedding materials, a bedding that has the least favorable thermal properties can limit the load capacity of the entire arrangement by reaching the maximum permitted conductor temperature (as in the real case). Therefore, it may not be possible to investigate all bedding materials up to the maximum permissible conductor temperatures without the potential of deteriorating the insulation materials. For instance, this is the case with the configurations installed in the main field, evidenced in the results presented. For the cable configurations in the main field, the loam bedding generally prevents the testing of the other beddings up to the permissible temperature limits. The ideal situation would be for each bedding to have a separate cable loop, although this would mean that simultaneous operation would only be possible with additional transformers. Depending on the specific experimental situation, certain compromises are probably unavoidable for its practical implementation.

Finally, when planning a corresponding field experiment, the relevant boundary conditions should always be taken into account and measured as accurately as possible. For the case of buried cables, particular changes in weather conditions lead to natural variations of the thermal and hydraulic situation in cable beddings [30]. Regarding the natural thermal situation, Figure 12 illustrates this issue with measurement values of the air and undisturbed soil temperatures in different depths over one calendar year at the test site. Depending on the thermal properties of the soil, there is an attenuation as well as a phase shift of the cyclic air temperature fluctuations with increasing depth. To estimate the periodic temperature fluctuations in the near-surface soil, the sinusoidal temperature oscillations for time periods of 24 h or 365 days can be assumed to be valid approximations [39]. Besides basic parameters such as air temperature and precipitation, the monitoring of further meteorological parameters is recommended, thereby allowing for an estimation of the potential evaporation. Depending on the experimental design, it might be necessary to consider the hydraulic influences of vegetation on the cable's surroundings.

Thus, if bare soils are not used, it should be taken into account that plants extract water from the soil via their root system, which influences the overall hydraulic situation in the shallow subsurface. An adequate knowledge of these effective boundary conditions is crucial, particularly for more advanced simulation approaches of the heat transfer around shallow heat sources, such as buried power cables.

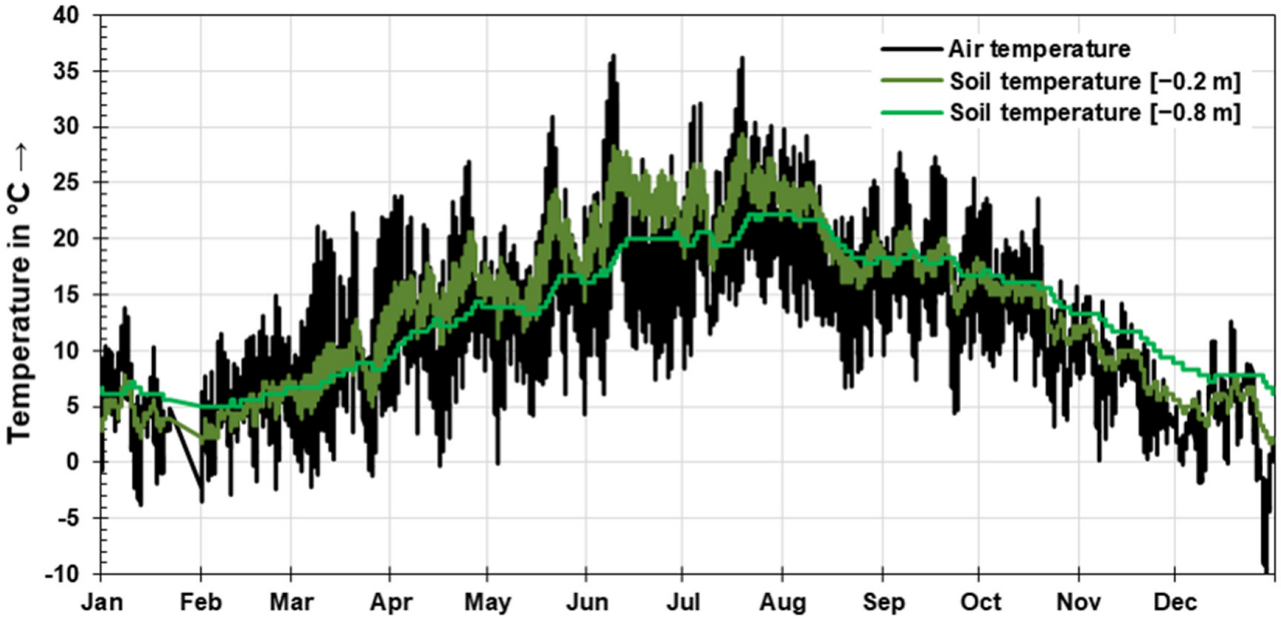

Figure 12. Measured air and undisturbed soil temperatures at the location of the weather station over one calendar year.

4.2. Influence of Bedding Materials on the Ampacity of Buried Power Cables

The presented experimental results emphasize the strong influences of different bedding materials on the conductor temperatures, respectively to the maximum cable ampacity. While the cable ampacity calculations according to the standards assume a homogeneous and isotropic medium around the cables, in practice, a cable trench usually has a heterogeneous structure and the thermal and hydraulic properties of the materials may differ considerably. Furthermore, a variety of interactions occur between the surrounding soil and the bedding body due to their hydraulic and thermal contact. As a result, the hydraulic and thermal properties of the soil and the cable bedding, which are decisive for the cable ampacity, are subject to natural (weather-related) and operational changes. For example, as in the case of the measured values shown in Figures 7 and 11, the effective thermal conductivity of the bedding can vary considerably as a result of precipitation events, although it should be noted that the sensitivity of a bedding material to these effects depends primarily on its hydraulic properties. In contrast, present standards assume, using a conservative approach, a steady state (permanent) of drying of the bedding in the vicinity of underground cables. Considering the strong seasonal fluctuation and high daily fluctuation of generations from renewable energy sources, the question as to whether and to what extent this applies to cable systems used to connect these facilities arises. Until now, there has not been any reliable information available on whether drying-out occurs at all during short-term high loads of cable systems or to what extent the bedding is regenerated by precipitation events or by a short-term thermal load reduction. Furthermore, the observed differences in the temporal duration of drying and rewetting effects might be important to consider. Another contributory factor is that drying processes around the cable may cause shrinkage processes of the bedding material, influencing the thermal contact of the cable to the bedding.

In particular, the presented results of the investigations of the main field cable configurations emphasize that areas with poor thermal properties might limit the transmission capacity of the entire cable route. In such cases, it may be practical to reinforce the network

through a selective use of highly thermally conductive bedding materials in at areas of critical points (such as intersections of different infrastructures). For existing unfilled protection pipe systems, subsequent backfilling with a grouting material might increase the possible maximum load and thus reduce the need for the construction of new cable routes. For distribution grids in particular, precise knowledge of the effective thermal properties of the bedding materials allows for an efficient utilization of grid resources and forms the basis of algorithms that control consumption and generation for the reliable and efficient use of renewable energies in a potential future smart grid. With regard to the operation of cable systems, critical grid conditions can be predicted with the additional knowledge of environmental conditions and their influence on the effective thermal behavior of the cable-bedding-soil system on the one hand, and the expected load on the cable on the other.

5. Conclusions

To investigate the heat dissipation processes around buried power cables in real scale and with realistic electric loading, a field experiment consisting of a main field with various cable configurations laid in four different bedding materials and a side field with additional cable trenches for thermal enhanced bedding materials and protection pipe systems was planned and constructed. The presented test configurations allow for an application of constant as well as dynamic load profiles on the cables in the test site, whereas further important boundary conditions such as the hydraulic situation were monitored, alongside the temperatures.

The experimental results reveal that the performance of buried cable systems strongly depend on the effective thermal properties of the surrounding bedding material. For example, the loam bedding presented the least favorable heat dissipation properties and thus the highest conductor temperatures in all of the main field measurement results presented. Significant drying and rewetting effects were only found for the sand bedding, which therefore possessed the strongest variations in the measured conductor temperatures as observed. In general, the sensitivity of a bedding material to these effects depends primarily on its hydraulic properties. For the ducted systems the use of artificial grouting materials within the protection pipes leads to an increase in ampacity between 25% and 35%, which is especially pronounced for dynamic load scenarios. All of these results highlight that those areas with poor thermal properties limit the transmission capacity of the entire cable route, and a more precise understanding of thermal properties of the cable bedding would be beneficial for future applications such as smart grid infrastructure.

Author Contributions: Conceptualization, C.V.-D. and I.S.; construction of test site, C.V.-D.; operation of test site, data acquisition and evaluation, C.V.-D., M.S. and C.B.; simulation, C.B.; writing—original draft preparation, C.V.-D. and M.S.; writing—review and editing, C.V.-D., M.S., C.B., V.H. and I.S.; funding acquisition and supervision, V.H. and I.S. All authors have read and agreed to the published version of the manuscript.

Funding: This research was funded by the E.ON Innovation Center Distribution and the Bayernwerk AG. Parts of this work were also financially supported by the DFG in the framework of the Excellence Initiative, Darmstadt Graduate School of Excellence Energy Science and Engineering (GSC 1070) and by the Förderinitiative interdisziplinäre Forschung (fif) of the TU Darmstadt. We further acknowledge support by the Deutsche Forschungsgemeinschaft (DFG—German Research Foundation) and the Open Access Publishing Fund of Technical University of Darmstadt.

Institutional Review Board Statement: Not applicable.

Informed Consent Statement: Not applicable.

Data Availability Statement: The presented data from the conducted experiments and the investigated bedding materials are available online: https://doi.org/10.48328/tudatalib-665.

Acknowledgments: The authors thank J. Stegner for his support in the planning, construction and initial operation of the test site. Furthermore, the authors thank J. Hesse, H. Hoffmann, T. Rybak, P. Wiesner as well as S. Noll and R. Seehaus for their help during the construction of the field experiment. We would also like to thank HeidelbergCement AG for providing artificial bedding materials and supporting the installation of these materials. Valuable input regarding the calculation of the real cable losses by H. Janssen is also appreciated.

Conflicts of Interest: The authors declare no conflict of interest.

References

1. Toman, M.T.; Jemelkova, B. Energy and Economic Development: An Assessment of the State of Knowledge. *Energy J.* **2003**, *24*, 93–122. [CrossRef]
2. Editorial The greener grid. *Nature* **2008**, *454*, 551–552. [CrossRef]
3. Steinbach, A. Barriers and solutions for expansion of electricity grids—The German experience. *Energy Policy* **2013**, *63*, 224–229. [CrossRef]
4. Bertsch, V.; Hall, M.; Weinhardt, C.; Fichtner, W. Public acceptance and preferences related to renewable energy and grid expansion policy: Empirical insights for Germany. *Energy* **2016**, *114*, 465–477. [CrossRef]
5. Lienert, P.; Sütterlin, B.; Siegrist, M. Public acceptance of high-voltage power lines: The influence of information provision on undergrounding. *Energy Policy* **2018**, *112*, 305–315. [CrossRef]
6. Menges, R.; Beyer, G. Underground cables versus overhead lines: Do cables increase social acceptance of grid development? Results of a Contingent Valuation survey in Germany. *Int. J. Sustain. Energy Plan. Manag.* **2014**, *3*, 33–48. [CrossRef]
7. Forschungsgemeinschaft für Elektrische Anlagen und Stromwirtschaft. In *Planungshandbuch zur Integration von Erzeugungsanlagen in Verteilungsnetze*; FGH: Mannheim, Germany, 2014.
8. Anders, G.J. *Rating of Electric Power Cables: Ampacity Computations for Transmission, Distribution, and Industrial Applications*, 1st ed.; McGraw-Hill Professional: New York, NY, USA, 1997; 428p.
9. Neher, J.H.; McGrath, M.H. The calculation of the temperature rise and load capability of cable systems. *Trans. Am. Inst. Electr. Eng. Part III Power Appar. Syst.* **1957**, *76*, 752–764. [CrossRef]
10. *IEC 60287 Electric Cables—Calculation of the Current Rating*; International Electrotechnical Committee: Geneva, Switzerland, 2014.
11. *IEC 60853 Calculation of the Cyclic and Emergency Current Rating of Cables*; International Electrotechnical Committee: Geneva, Switzerland, 2008.
12. Brakelmann, H. *Physical Principles and Calculation Methods of Moisture and Heat Transfer in Cable Trenches*, 1st ed.; VDE: Berlin, Germany, 1984; 93p.
13. Philip, J.R.; De Vries, D.A. Moisture movement in porous materials under temperature gradients. *Trans. Am. Geophys. Union* **1957**, *38*, 222–232. [CrossRef]
14. CIGRE 21 Current ratings of cables buried in partially dried out soil. *Electra* **1986**, *104*, 12–22.
15. CIGRE 21 Methods for calculating cyclic ratings for buried cables with partial drying of the surrounding soil. *Electra* **1992**, *145*, 32–67.
16. CIGRE 21 Determination of a value of critical temperature rise for a cable backfill material. *Electra* **1992**, *145*, 14–30.
17. Campbell, G.S.; Norman, J.M. *An Introduction to Environmental Biophysics*, 2nd ed.; Springer: New York, NY, USA, 1998. [CrossRef]
18. Blume, H.-P.; Brümmer, G.W.; Fleige, H.; Horn, R.; Kandeler, E.; Kögel-Knabner, I.; Kretzschmar, R.; Stahr, K.; Wilke, B.-M. *Scheffer/Schachtschabel Soil Science*, 1st ed.; Springer: Berlin/Heidelberg, Germany, 2016. [CrossRef]
19. Saito, H.; Šimůnek, J.; Mohanty, B.P. Numerical Analysis of Coupled Water, Vapor, and Heat Transport in the Vadose Zone. *Vadose Zone J.* **2006**, *5*, 784–800. [CrossRef]
20. Moradi, A.; Smits, K.M.; Lu, N.; McCartney, J.S. Heat Transfer in Unsaturated Soil with Application to Borehole Thermal Energy Storage. *Vadose Zone J.* **2016**, *15*, 1–17. [CrossRef]
21. Verschaffel-Drefke, C.; Balzer, C.; Schedel, M.; Hinrichsen, V.; Sass, I. Experiment for Validation of Numerical Models of Coupled Heat and Mass Transfer around Energy Cables. *VZJ* **2021**. [CrossRef]
22. Campbell, G.S.; Jungbauer, J.D.; Bidlake, W.R.; Hungerford, R.D. Predicting the effect of temperature on soil thermal conductivity. *Soil Sci.* **1994**, *158*, 307–313. [CrossRef]
23. Côté, J.; Konrad, J.-M. A generalized thermal conductivity model for soils and construction materials. *Can. Geotech. J.* **2005**, *42*, 443–458. [CrossRef]
24. Ocłoń, P.; Cisek, P.; Pilarczyk, M.; Taler, D. Numerical simulation of heat dissipation processes in underground power cable system situated in thermal backfill and buried in a multilayered soil. *Energy Convers. Manag.* **2015**, *95*, 352–370. [CrossRef]
25. Kroener, E.; Campbell, G.S.; Bittelli, M. Estimation of Thermal Instabilities in Soils around Underground Electrical Power Cables. *Vadose Zone J.* **2017**, *16*, 1–13. [CrossRef]
26. Hruška, M.; Clauser, C.; De Doncker, R.W. Influence of dry ambient conditions on performance of underground medium-voltage DC cables. *Appl. Therm. Eng.* **2018**, *149*, 1419–1426. [CrossRef]
27. Trüby, P.; Aldinger, E. Auswirkungen der Wärmeemission von Hochspannungserdkabeln auf den Wärme- und Wasserhaushalt des Bodens. *Schr.-R.D. Dtsch. Rates Für Landespfl.* **2013**, *84*, 100–108.

28. Mitchell, J.K.; McMillan, J.C.; Green, S.L.; Sisson, R.C. Field Testing of Cable Backfill Systems. In Proceedings of the Symposium on Underground Cable Thermal Backfill, Toronto, ON, Canada, 17–18 September 1981; pp. 19–32.
29. Radhakrishna, H.S. Fluidized Cable Thermal Backfill. In Proceedings of the Symposium on Underground Cable Thermal Backfill, Toronto, ON, Canada, 17–18 September 1981; pp. 34–53.
30. Koopmans, G.; van de Wiel, G.M.L.M.; van Loon, L.J.M.; Palland, C.L. Soil physical route survey and cable thermal design procedure. *IEE Proc. C Gener. Transm. Distrib.* **1989**, *136*, 341–346. [CrossRef]
31. Gouda, O.E.; Abdel-Aziz, A.M.; Refale, R.A.; Matter, Z. Experimental study for drying-out of soil around underground power cables. In Proceedings of the 5th Midwest Symposium on Circuits and Systems, Washington, DC, USA, 9–12 August 1992; pp. 99–102. [CrossRef]
32. Trinks, S.; Kluge, B.; Wessolek, G.; Köhler, M. Optimierung der Strombelastbarkeit erdverlegter Energiekabel—Ein neues Berechnungsverfahren CableEarth. *Netzpraxis* **2013**, *52*, 51–58.
33. Trüby, P. *Auswirkungen der Wärmeemission von Höchstspannungserdkabeln auf den Boden und auf Landwirtschaftliche Kulturen*; Consentec GmbH: Berlin, Germany, 2014; 45p.
34. Stegner, J.; Drefke, C.; Hentschel, K.; Sass, I. Quantifizierung der Wärmeableitung bei erdverlegten Mittel- und Niederspannungskabeln. *BBR* **2013**, *64*, 16–21.
35. *HLNUG Bodenkarte von Hessen 1:25000—Blatt 6117 Darmstadt West*, 1st ed.; Hessian Agency for Nature Conservation, Environment and Geology: Wiesbaden, Germany, 1985.
36. *HLNUG Geologische Übersichtskarte von Hessen 1:300000*, 5th ed.; Hessian Agency for Nature Conservation, Environment and Geology: Wiesbaden, Germany, 2007.
37. *DIN VDE 0276-1000 Starkstromkabel-Teil 1000: Strombelastbarkeit, Allgemeines, Umrechnungsfaktoren*; Beuth Publishing DIN: Berlin, Germany, 1995.
38. Drefke, C.; Schedel, M.; Stegner, J.; Balzer, C.; Hinrichsen, V.; Sass, I. Measurement Method of Thermal Properties of Cementitious Bedding Materials and Unsaturated Soils: Hydraulic Influence on Thermal Parameters. *GTJ* **2017**, *40*, 160–170. [CrossRef]
39. Kirkham, D.; Powers, W.L. *Advanced Soil Physics*; Wiley-Interscience: Hoboken, NJ, USA, 1972; 534p.